

Research Article

Efficient Control Charting Scheme for the Process Location with Application in Automobile Industry

Syed Masroor Anwar ¹, Somayya Komal ², Ammara Nawaz Cheema ²,
Nafiu Lukman Abiodun ³, Zahid Rasheed ⁴, and Majid Khan ⁵

¹Department of Statistics, University of Azad Jammu and Kashmir, Muzaffarabad, Pakistan

²Department of Mathematics, Air University, Islamabad, Pakistan

³Department of Economics and Statistics, Faculty of Economics and Management Sciences Kabale University, Kabale, Uganda

⁴Department of Mathematics, Women University of Azad Jammu and Kashmir, Bagh, Pakistan

⁵Government Post Graduate College for Boys, Haripur, Pakistan

Correspondence should be addressed to Nafiu Lukman Abiodun; lanafiu@kab.ac.ug

Received 23 April 2022; Accepted 6 September 2022; Published 15 October 2022

Academic Editor: Tahir Mehmood

Copyright © 2022 Syed Masroor Anwar et al. This is an open access article distributed under the Creative Commons Attribution License, which permits unrestricted use, distribution, and reproduction in any medium, provided the original work is properly cited.

The recently introduced triple exponentially weighted moving average (TEWMA) chart is the extended form of the classical EWMA and double EWMA (DEWMA) charts. On the other hand, the auxiliary information-based (AIB) homogeneously weighted moving average ($HWMA_{AIB}$) chart is used for the monitoring of process location shifts efficiently as compared to the HWMA chart. Combining TEWMA with HWMA features is a new idea and is not seen in the literature until now. So, the objective of this study is to combine the idea of $HWMA_{AIB}$ and TEWMA charts and propose an AIB triple HWMA, symbolized as $THWMA_{AIB}$ chart to further improve the process location shift monitoring. The proposed $THWMA_{AIB}$ chart is developed by combining the AIB double HWMA plotting statistic into the other HWMA chart. The numerical results are computed using the Monte Carlo simulation method. Average run length (ARL), relative ARL, performance comparison index, and extra quadratic loss are used as comparison tools for the proposed $THWMA_{AIB}$ chart with the classical EWMA, TEWMA, mixed HWMA-CUSUM (MHC), AIB EWMA ($EWMA_{AIB}$), HWMA, double HWMA (DHWMA), $HWMA_{AIB}$, AIB mixed EWMA-CUSUM (MEC_{AIB}), and AIB mixed CUSUM-EWMA (MCE_{AIB}) charts. Finally, a practical application is also provided for users to demonstrate the proposed study's vitality.

1. Introduction

Variations are an integral part of all kinds of production and non-production processes. These variations are categorized as common and special variations. Generally, these special variations can result in process parameters (location and/or dispersion) shifts. These shifts are classified into three sizes as small, moderate, and large. Control charts are widely used in the statistical process control (SPC) toolkit to identify these special variations. For tracking large shifts, Shewhart charts [1] are widely used; however, for small to moderate shifts, cumulative sum (CUSUM) [2] and exponentially weighted moving average (EWMA) [3] are used.

In the SPC literature, many enhancements and modifications on control charts continuously fulfil the practitioner's requirement of quickly detecting shifts. In this regard, Shamma and Shamma [4] extended the classical EWMA chart and suggested an improved double EWMA (DEWMA) chart. The DEWMA chart is more responsive than the classical EWMA chart. Alevizakos, et al. [5] proposed a triple EWMA (TEWMA) chart, the extended version of the EWMA and DEWMA charts for process location. The TEWMA chart is handy for detecting smaller process location shifts. After that, Alevizakos, et al. [6] recommended one-sided and two-sided TEWMA charts for the time between events, regarded as $TEWMA_{TBE}$ charts, and

showed that the TEWMA_{TBE} charts are more sensitive than the DEWMA_{TBE} and EWMA_{TBE} charts. Similarly, Sukparungsee, et al. [7], Taboran, et al. [8], and Talordphop, et al. [9] suggested mixed EWMA-moving average (MA), Tukey MA-DEWMA, modified EWMA-MA control charts for process location, respectively. Also, Taboran, et al. [10] introduced non-parametric Tukey MA-EWMA control chart for detecting process location shifts. To monitor process dispersion, Chatterjee, et al. [11] developed a TEWMA chart using three parameters of logarithmic transformation to S^2 and named as S^2 -TEWMA chart. Subsequently, Alevizakos, et al. [12] formulated a non-parametric TEWMA sign chart for process median. Recently, Alevizakos, et al. [13] suggested non-parametric TEWMA sign ranked charts. Similarly, Rasheed, et al. [14] introduced Nonparametric Triple EWMA Wilcoxon Signed-Rank Control Chart for process location.

Similarly, using auxiliary information with the original study variable enhances the control chart's detection ability [15]. Many researchers identified various features of the auxiliary information-based (AIB) memory charts. For illustration, Abbas, et al. [16] initiated an AIB EWMA (EWMA_{AIB}) chart to monitor process location. Likewise, Adegoke, et al. [17] introduced an AIB EWMA chart for monitoring process location shifts using various sampling schemes. Similarly, Noor-ul-Amin, et al. [18] presented the AIB HEWMA (HEWMA_{AIB}) chart for the phase-II process monitoring of the location parameter. Abbasi and Haq [15] recommended AIB optimal and adaptive CUSUM chart for process location. Similarly, Haq and Khoo [19] designed the AIB multivariate chart for the mean vector. Subsequently, Anwar, et al. [20] and Aslam and Anwar [21] provided AIB modified-EWMA and Bayesian modified-EWMA charts to improve process location monitoring. Also, to monitor process location, Anwar, et al. [22] formulated two new charts using auxiliary information named mixed EWMA-CUSUM (MCE_{AIB}) and mixed CUSUM-EWMA (MEC_{AIB}) charts. Recently, a combined MEC_{AIB} chart is proposed for the simultaneous monitoring of process location and dispersion parameters [23]. Haq, et al. [24] suggested adaptive CUSUM and EWMA under variable sampling intervals using auxiliary information. More details of AIB memory charts are available in Lee, et al. [25], Haq [26], Haq [27], Adegoke, et al. [28] and the references therein.

Hunter [29] points out the drawback of classical EWMA statistic is that the freshest observations are given more weight than previous observations. To resolve this drawback, Abbas [30] proposed a homogeneous weighted moving average (HWMA) chart that assigns particular weights to recent process values and homogeneously allocates the remaining weights to the old process values. This approach enhances the effectiveness of the HWMA chart as compared to its competitor's charts. Later Adegoke, et al. [28] extended the Abbas [30] work to propose the AIB HWMA (HWMA_{AIB}) chart is more effective for smaller shift monitoring. Subsequently, Adeoti and Koleoso [31] and Abid, et al. [32] enhanced the existing work by introducing a hybrid-HWMA (HHWMA) and double HWMA

(DHWMA) charts, respectively. Also, Thanwane, et al. [33] presented an HWMA chart for the autocorrelated process under the assumption of estimated parameters. Unlike process location monitoring, Riaz, et al. [34] utilized the HWMA chart concept for efficient process dispersion monitoring. Recently, Abid, et al. [35] introduced a mixed HWMA-CUCUM (MHC) chart for process location for efficient process monitoring. Also, Rasheed, et al. [36] introduced homogeneously mixed memory control chart for process location.

Motivated by the extraordinary performances of TEWMA and HWMA_{AIB} charts, we are aimed to combine the features of TEWMA and HWMA_{AIB} charts and proposed a more efficient AIB triple HWMA (symbolized as (THWMA_{AIB})) chart for process location. The merging of TEWMA with HWMA features in the presence of auxiliary information is a new idea and is not seen in the literature till now and it is expected that the combining of TEWMA and HWMA_{AIB} charts features will further boost the performance of proposed THWMA_{AIB} chart. Average run length (ARL), relative ARL (RARL), extra quadratic loss (EQL), and performance comparison index (PCI) are used for the performance comparison with existing counterparts. Besides, the Monte Carlo simulation method is used for obtaining numerical measures. The classical EWMA, TEWMA, MHC, EWMA_{AIB}, HWMA, DHWMA, HWMA_{AIB}, MEC_{AIB}, and MCE_{AIB} charts are considered for the comparison. Additionally, the proposed THWMA_{AIB} chart is implemented in a real-world scenario to demonstrate its utility in practice.

The remainder of the research article is structured as follows: existing charts are described in Section 2. Additionally, Section 3 enlisted the design structure and special cases of proposed (THWMA_{AIB}) chart. Furthermore, the next section provides the performance evaluation and comparison against classical EWMA, TEWMA, MHC, EWMA_{AIB}, HWMA, HWMA_{AIB}, DHWMA, MEC_{AIB}, and MCE_{AIB} charts. Also, the application of (THWMA_{AIB}) chart is included in Section 5. The last section describes the overall summary, conclusions, and recommendations.

2. Existing Methods

This section describes the detailed methodology of the existing HWMA_{AIB} and TEWMA charts for process location monitoring.

2.1. Variable of Interest and Auxiliary Information. Assume that the process variable Y is normally distributed with a mean $\mu_Y + \delta\sigma_Y$ and variance σ_Y^2 . Let $\bar{Y}_t = \sum_{i=1}^n Y_{it}/n$ and $S_{Yt}^2 = \sum_{i=1}^n (Y_{it} - \bar{Y}_t)^2/(n-1)$ represents the sample mean and variance of Y of size n . If $\delta = 0$, the process is in-control (IC); otherwise, it is out-of-control (OOC). So, for the IC situation, \bar{Y}_t and S_{Yt}^2 are mutually independent identically distributed. Let X be an auxiliary variable of Y . The X and Y follow a bivariate normal distribution (BND) (i.e., $(Y, X) \sim N(\mu_Y, \mu_X, \sigma_Y, \sigma_X, \rho)$, where μ_X represents the mean and σ_X represents the standard deviation of X . Also,

the ρ is the correlation coefficient corresponding to X and Y . The AIB regression estimator for process location is given as follows:

$$R_t = \bar{Y}_t + b_{YX}(\mu_X - \bar{X}_t), \quad (1)$$

where, $b_{YX} = \rho(\sigma_Y/\sigma_X)$, $E(R_t) = \mu_Y$ and $\text{Var}(R_t) = \sigma_Y^2 - b_{YX}^2\sigma_X^2/n$.

2.2. **HWMA_{AIB} Chart.** Adegoke, et al. [28] introduced HWMA_{AIB} chart to track changes in process location. The

HWMA_{AIB} chart is the extended form of HWMA chart, used when interest variable is observed along with auxiliary information variable. The plotting statistic of the HWMA chart given as:

$$H_t = \lambda_1 R_t + (1 - \lambda_1)\bar{R}_{t-1}, \quad (2)$$

where \bar{Y}_t is the sample average of t^{th} sample and $\lambda_1 \in (0, 1]$ is the smoothing constant, and $\bar{R}_{t-1} = \sum_{i=1}^{t-1} R_i / t - 1$ is the mean of preceding $t - 1$ observations The control limits of the HWMA_{AIB} chart are:

$$\left. \begin{aligned} LCL_{(HWMA_{AIB})t} &= \begin{cases} \mu_0 - L_{HWMA_{AIB}} \sigma_Y \sqrt{(\lambda^2/n)(1 - \rho^2)}, & \text{if } t = 1 \\ \mu_0 - L_{HWMA_{AIB}} \sigma_Y \sqrt{\frac{1}{n} \left\{ \lambda^2 + \frac{(1 - \lambda)^2}{(t - 1)} \right\} (1 - \rho^2)}, & \text{if } t > 1 \end{cases} \\ UCL_{(HWMA_{AIB})t} &= \begin{cases} \mu_0 + L_{HWMA_{AIB}} \sigma_Y \sqrt{(\lambda^2/n)(1 - \rho^2)}, & \text{if } t = 1 \\ \mu_0 + L_{HWMA_{AIB}} \sigma_Y \sqrt{\frac{1}{n} \left\{ \lambda^2 + \frac{(1 - \lambda)^2}{(t - 1)} \right\} (1 - \rho^2)}, & \text{if } t > 1 \end{cases} \end{aligned} \right\} \quad (3)$$

The $L_{HWMA_{AIB}}$ represents the coefficient of control limits. If $H_t > UCL_{(HWMA_{AIB})t}$ or $H_t < LCL_{(HWMA_{AIB})t}$, the process is OOC; otherwise, IC.

2.3. **TEWMA Chart.** Alevizakos et al. [5] designed a TEWMA chart for efficient process location monitoring. The plotting statistics of the TEWMA chart are defined as

$$\begin{cases} E_t = \lambda Y_t + \lambda E_{t-1}, \\ DE_t = \lambda E_t + \lambda DE_{t-1}, \\ TE_t = \lambda DE_t + \lambda TE_{t-1}, \end{cases} \quad (4)$$

where $\lambda \in (0, 1]$ is a TEWMA constant. The initial values of E_0, DE_0, TE_0 are all equal to μ_0 . The mean and variance of the TE_t are $E(TE_t) = \mu_0$ and

$$\begin{aligned} \text{var}(TE_t)/\sigma^2 &= \theta^3 \lambda^6 / 4 \left[-\{t(t^2 - 1)(t - 2)\theta^{-3}/1 - \theta\} - 4\{t(t^2 - 1)\theta^{-2}/(1 - \theta^2)\} - 12\{t(t + 1)\theta^{-1}/(1 - \theta^3)\} - 24\{(t + 1)\theta/(1 - \theta^4)\} + 24\{(1 - \theta^{t+1})/(1 - \theta^5)\} \right] \\ &+ 2\theta^2 \lambda^6 \left[-\{t(t^2 - 1)\theta^{-2}/1 - \theta\} - 3\{t(t + 1)\theta^{-1}/(1 - \theta^2)\} - 6\{(t + 1)\theta/(1 - \theta^3)\} + 6\{(1 - \theta^{t+1})/(1 - \theta^4)\} \right] \\ &+ 7\theta \lambda^6 / 2 \left[-\{t(t + 1)\theta^{-1}/1 - \theta\} - 2(t + 1)\theta/(1 - \theta^2) + \{2(1 - \theta^{t+1})/(1 - \theta^3)\} \right] \\ &+ \lambda^6 \left[\{(1 - \theta^{t+1})/(1 - \theta^2)\} - \{(t + 1)\theta/(1 - \theta)\} \right], \end{aligned} \quad (5)$$

respectively, where $\theta = (1 - \lambda)^2$. The time-varying control limits of the TEWMA chart are defined as:

$$\begin{cases} LCL_{(TEWMA)t} = \mu_0 - L_{TEWMA} \sqrt{\text{var}(TE_t)}, \\ UCL_{(TEWMA)t} = \mu_0 + L_{TEWMA} \sqrt{\text{var}(TE_t)}, \end{cases} \quad (6)$$

where L_{TEWMA} ($L_{TEWMA} > 0$) is the control limits coefficient of the TEWMA chart. The process will be OOC if any $TE_t > UCL_{(TEWMA)t}$ or $TE_t < LCL_{(TEWMA)t}$.

3. Proposed Method

The methodology for the proposed chart is described in this section. Subsection 3.1 covers the design structure of the proposed THWMA_{AIB} chart. Besides, the special cases of the THWMA_{AIB} chart are given in Subsection 3.2.

3.1. **Proposed THWMA_{AIB} Chart.** To construct the proposed THWMA_{AIB} chart, the plotting statistic of the THWMA_{AIB} chart is given as:

$$H_t = \lambda_1 R_t + (1 - \lambda_1) \bar{R}_{t-1}, \tag{7}$$

$$DH_t = \lambda_2 H_t + (1 - \lambda_2) \bar{R}_{t-1}, \tag{8}$$

$$TH_t = \lambda_3 DH_t + (1 - \lambda_3) \bar{R}_{t-1}. \tag{9}$$

We assume $\lambda_1 = \lambda_2 = \lambda_3 = \lambda$ by following Shamma and Shamma [4] and Abid, et al. [32], then after simplification, the TH_t statistic can be written as:

$$TH_t = \lambda^3 R_t + (1 - \lambda^3) \bar{R}_{t-1}. \tag{10}$$

The TH_t statistic in Equation (9) can be expressed as:

$$TH_t = \lambda^3 R_t + \left[\left(\frac{1 - \lambda^3}{i - 1} \right) R_{t-1} + \left(\frac{1 - \lambda^3}{i - 1} \right) R_{t-2} + \dots + \left(\frac{1 - \lambda^3}{i - 1} \right) R_1 \right]. \tag{11}$$

Also, for TH_t , $E(TH_t) = \mu_0$, $\text{var}(TH_t) = \lambda^6/n(1 - \rho^2) \sigma_Y^2$ for $t = 1$, $\text{var}(TH_t) = \lambda^6/n(1 - \rho^2) \sigma_Y^2 + (1 - \lambda^3)^2/n(t - 1)(1 - \rho^2) \sigma_Y^2$ for $t > 1$. The proposed $THWMA_{AIB}$ chart's control limits are written as:

$$LCL_{(THWMA_{AIB})t} = \left. \begin{aligned} & \mu_0 - L_{THWMA_{AIB}} \sigma_Y \sqrt{\frac{\lambda^6}{n} (1 - \rho^2)}, \quad \text{if } t = 1 \\ & \mu_0 - L_{THWMA_{AIB}} \sigma_Y \sqrt{\frac{1}{n} \left\{ \lambda^6 + \frac{(1 - \lambda^3)^2}{(t - 1)} \right\} (1 - \rho^2)}, \quad \text{if } t > 1 \\ & \mu_0 + L_{THWMA_{AIB}} \sigma_Y \sqrt{\frac{\lambda^6}{n} (1 - \rho^2)}, \quad \text{if } t = 1 \\ & \mu_0 + L_{THWMA_{AIB}} \sigma_Y \sqrt{\frac{1}{n} \left\{ \lambda^6 + \frac{(1 - \lambda^3)^2}{(t - 1)} \right\} (1 - \rho^2)}, \quad \text{if } t > 1 \end{aligned} \right\}, \tag{12}$$

where $L_{THWMA_{AIB}}$ is the control limits co-efficient. The TH_t statistic is plotted along with $LCL_{(THWMA_{AIB})t}$ and $UCL_{(THWMA_{AIB})t}$. The process is declared IC if $TH_t > LCL_{(THWMA_{AIB})t}$ or $TH_t < UCL_{(THWMA_{AIB})t}$; otherwise, OOC.

3.2. Special Cases of $THWMA_{AIB}$ Chart. The proposed $THWMA_{AIB}$ chart reduced to some existing charts including $HWMA$, $DHWMA$, and $HWMA_{AIB}$ charts by considering special values of parameters. The special cases, along with their proves, are provided here.

Case 1. When $\rho = 0$ and $\lambda_3 = 1$, the proposed $THWMA_{AIB}$ chart tends to the $DHWMA$ chart.

Proof. When $\rho = 0$, then the difference R_t estimator reduces to

$$R_t^{(1)} = \bar{Y}_t. \tag{13}$$

Now substitute the resulted $R_t^{(1)}$ in Equation (6) to obtain

$$H_t^{(1)} = \lambda_1 R_t^{(1)} + (1 - \lambda_1) R_{t-1}^{(1)}, \tag{14}$$

Then the Equation (7) can be written as

$$DH_t^{(1)} = \lambda_2 H_t^{(1)} + (1 - \lambda_2) R_{t-1}^{(1)}. \tag{15}$$

Now substitute Equation (14) in Equation (8) which provides the following:

$$TH_t^{(1)} = \lambda_3 DH_t^{(1)} + (1 - \lambda_3) R_{t-1}^{(1)}. \tag{16}$$

Also, put $\lambda_3 = 1$ in Equation (15) then the $TH_t^{(1)}$ reduced as follows:

$$TH_t^{(1)} = DH_t^{(1)}. \tag{17}$$

This shows that statistic of proposed $THWMA_{AIB}$ chart becomes the statistic of $DHWMA$ by Abid, et al. [32], when $\rho = 0$ and $\lambda_3 = 1$. \square

Case 2. The proposed $THWMA_{AIB}$ chart converts to $THWMA$ chart at $\rho = 0$.

Proof. Consider estimator $R_t^{(1)}$ which is given in Equation (12) when $\rho = 0$ (i.e., $R_t^{(1)} = \bar{Y}_t$). Based on $R_t^{(1)}$, the $H_t^{(1)}$ of Equation (13) will be as follows:

$$H_t^{(1)} = \lambda_1 R_t^{(1)} + (1 - \lambda_1) R_{t-1}^{(1)}. \tag{18}$$

Substituting the $H_t^{(1)}$ in the plotting statistic of the DH_t , (presented as $DH_t^{(2)}$ in this case) we get:

$$DH_t^{(2)} = \lambda_2 H_t^{(1)} + (1 - \lambda_2) R_{t-1}^{(1)}, \quad (19)$$

$$TH_t^{(2)} = \lambda_3 DH_t^{(1)} + (1 - \lambda_3) R_{t-1}^{(1)}. \quad (20)$$

The $TH_t^{(2)}$ in Equation (20) is the THWMA chart with no correlation. Hence, the proposed THWMA_{AIB} chart reduced to the statistic of the THWMA chart for $\rho = 0$. \square

Case 3. When $\lambda_2 = 1$ and $\lambda_3 = 1$, the proposed THWMA_{AIB} chart tends to the HWMA_{AIB} chart.

Proof. When $\lambda_2 = 1$ and $\lambda_3 = 1$, then the plotting statistic of the proposed THWMA_{AIB} chart, symbolized as $TH_t^{(3)}$ can be written as

$$TH_t^{(3)} = \lambda_1 R_t + (1 - \lambda_1) R_{t-1}. \quad (21)$$

The $TH_t^{(3)}$ in Equation (19) is similar to the HWMA_{AIB} statistic proposed by Adegoke, et al. [28] except for their notations. Hence, the statistic of proposed THWMA_{AIB} chart becomes the statistic of HWMA_{AIB} when $\lambda_2 = 1$ and $\lambda_3 = 1$. \square

Case 4. The proposed THWMA_{AIB} chart converts to the HWMA chart at $\rho = 0$, $\lambda_2 = 1$, and $\lambda_3 = 1$.

Proof. Consider estimator $R_t^{(1)}$ which is given in Equation (12) when $\rho = 0$ (i.e., $R_t^{(1)} = \bar{Y}_t$). Based on $R_t^{(1)}$, the $H_t^{(1)}$ of Equation (13) will be as follows:

$$H_t^{(4)} = \lambda_1 R_t^{(1)} + (1 - \lambda_1) R_{t-1}^{(1)}. \quad (22)$$

Substituting the $H_t^{(1)}$ in the plotting statistic of Equation (7) and (8), we get

$$\begin{aligned} DH_t^{(4)} &= \lambda_2 H_t^{(4)} + (1 - \lambda_2) R_{t-1}^{(1)}, \\ TH_t^{(4)} &= \lambda_3 DH_t^{(4)} + (1 - \lambda_3) R_{t-1}^{(1)}. \end{aligned} \quad (23)$$

Now put $\lambda_2 = 1$ and $\lambda_3 = 1$, then the plotting statistic of the proposed THWMA_{AIB} chart, symbolized as $TH_t^{(4)}$ can be written as

$$TH_t^{(4)} = \lambda_1 R_t^{(1)} + (1 - \lambda_1) R_{t-1}^{(1)}. \quad (24)$$

The $TH_t^{(4)}$ in Equation (22) is identical to the HWMA statistic. This shows that the THWMA_{AIB} chart is identical to the HWMA chart by Abbas (2018) for $\rho = 0$, $\lambda_2 = 1$, and $\lambda_3 = 1$. \square

Case 5. When $\lambda_3 = 1$, the proposed THWMA_{AIB} chart tends to the double HWMA_{AIB} (DHWMA_{AIB}) chart.

Proof. When $\lambda_3 = 1$, then the plotting statistic of the proposed THWMA_{AIB} chart, symbolized as $TH_t^{(5)}$ can be written as

$$TH_t^{(5)} = \lambda_2 DH_t + (1 - \lambda_2) R_{t-1}. \quad (25)$$

The $TH_t^{(5)}$ in Equation (23) is a DHWMA_{AIB} statistic. Hence, the statistic of proposed THWMA_{AIB} chart becomes the statistic of DHWMA_{AIB} for $\lambda_3 = 1$. \square

4. Performance Evaluation Measures

This section introduces the performance evaluation measures to analyze the charts' performance. The Monte Carlo simulation detail is given in Subsection 4.1. Likewise, the description of the ARL is enlisted in Subsection 4.2. Similarly, the overall performance evaluation measures are defined in Subsection 4.3. The choices of parameters of the proposed THWMA_{AIB} chart is given in Subsection 4.4.

4.1. Monte Carlo Simulation. The Monte Carlo simulation procedure is regarded as a computational technique for obtaining numerical results for evaluating the performance of the proposed THWMA_{AIB} chart. Monte Carlo simulation with 10^5 iterations is conducted for each displacement of δ using R software to obtain the ARL of the proposed THWMA_{AIB} chart. The shift is reflected in the process mean as: μ_Y to $\mu_Y + \delta\sigma_Y$, where $\delta = 0.00, 0.05, 0.10, 0.20, 0.25, 0.50, 1.00, 1.50, 2.00, 2.50, 3.00,$ and 5.00 . The proposed THWMA_{AIB} chart is constructed by following given below guidelines:

- (i) Generate random observations from $(Y_{it}, X_{it}) \sim N(\mu_Y, \mu_X, \sigma_Y, \sigma_X, \rho)$ ($t = 1, 2, 3, \dots$).
- (ii) Calculate the R_t estimator from Equation (1).
- (iii) Calculate the H_t statistics of the THWMA_{AIB} chart from Equation (6) using R_t estimator.
- (iv) Use the DH_t statistic as an input in Equation (8) to obtain the TH_t statistic.
- (v) Chose $L_{\text{THWMA}_{\text{AIB}}}$ along with other desired parameters (λ, ρ) for desired IC ARL denoted as ARL_0 .
- (vi) Compute $LCL_{(\text{THWMA}_{\text{AIB}})_t}$ and $UCL_{(\text{THWMA}_{\text{AIB}})_t}$ based on $L_{\text{THWMA}_{\text{AIB}}}$ and λ .
- (vii) Plot the TH_t statistic against the $LCL_{(\text{THWMA}_{\text{AIB}})_t}$ and $UCL_{(\text{THWMA}_{\text{AIB}})_t}$.
- (viii) If $TH_t > UCL_{(\text{THWMA}_{\text{AIB}})_t}$ or $TH_t < LCL_{(\text{THWMA}_{\text{AIB}})_t}$, record sequence order which is called run length (RL).
- (ix) Repeat steps (i)-(viii) 10^5 times.
- (x) Calculate the average of 10^5 RL, which is ARL_0 . If it is desired ARL_0 ; otherwise, adjust the L_{Proposed} accordingly and repeat from steps (i)-(ix) until will not get desired ARL_0 .
- (xi) For OOC ARL values, considered $(Y_{it}, X_{it}) \sim N(\mu_Y + \delta\sigma_Y, \mu_X)$, $(\sigma_Y, \sigma_X, \rho)$ and repeat from steps (ii)-(x).

4.2. Individual Performance Measure. The average run length (ARL) is commonly used to evaluate a chart's performance at a single shift. The ARL is listed as IC ARL (ARL_0) and OOC ARL (ARL_1). For IC state, the ARL_0

is chosen to be sufficiently large to eliminate the effect of the false alarm rate. On the other hand, the ARL_1 should be small enough to detect a shift quickly. A chart is preferred than the other competing charts if it should have a smaller ARL_1 value at predefined ARL_0 .

4.3. Overall Performance Evaluation Measures. The EQL, RARL, and PCI performance evaluation measures are used to evaluate a chart's overall effectiveness. More information can be found here.

The EQL is the weighted average ARL over the domain of shifts with δ^2 as a weight [37]. It is defined as:

$$EQL = (\delta_{\max} - \delta_{\min})^{-1} \int_{\delta_{\min}}^{\delta_{\max}} \delta^2 ARL(\delta) d\delta, \quad (26)$$

where $ARL(\delta)$ is the ARL at specific δ ; δ_{\min} and δ_{\max} are the smallest and largest shift values of the domain, respectively. The lower the EQL value signifies, the better the chart's performance.

The RARL, like EQL is also used to assess the efficiency of a chart. It can be defined as follows:

$$RARL = (\delta_{\max} - \delta_{\min})^{-1} \int_{\delta_{\min}}^{\delta_{\max}} \frac{ARL(\delta)}{ARL^*(\delta)} d\delta. \quad (27)$$

The $ARL(\delta)$ is the ARL of the competing chart. The $ARL^*(\delta)$ is the ARL of benchmark chart at a δ . A chart is decided as a benchmark chart for a smaller ARL at specific δ [22]. The RARL value of the benchmark chart is assumed to be one. If the competing chart has $RARL > 1$, the benchmark chart is more efficient than competing.

The PCI corresponds to the EQL ratio of the specific chart to the EQL of the benchmark chart. Here EQL^* represents the EQL of the benchmark chart, whereas the EQL represents the EQL of the competing chart. According to Ou, et al. [38], the PCI is presented as:

$$PCI = \frac{EQL}{EQL^*}. \quad (28)$$

The PCI of the benchmark chart should be one. If the $PCI > 1$, the benchmark chart is superior against the competing chart [20].

4.4. Effect of Parameters Choices. The design parameters ($\lambda, L_{THWMA_{AIB}}$) of the proposed $THWMA_{AIB}$ chart has its effect on the detection ability. Various combinations of these parameters are chosen, and hence corresponding ARL, the standard deviation of RL (SDRL), and median of RL (MDRL) are computed. The parameter λ is set as 0.10, 0.25, 0.50, and 0.75 to find the values of $L_{THWMA_{AIB}}$, to obtain $ARL_0 = 500$. Various ρ like 0.00, 0.25, 0.50, 0.75, and 0.95 are assumed for this study. Numerical results of the proposed $THWMA_{AIB}$ chart are presented in Tables 1–4.

5. Evaluation and Performance Comparison

This section presents comprehensive comparisons of the proposed $THWMA_{AIB}$ chart with classical EWMA [3], $EWMA_{AIB}$ [16], $HWMA$ [30], $HWMA_{AIB}$ [28], $DHWMA$ [32], $TEWMA$ [5], MCE_{AIB} and MEC_{AIB} [22], and MHC [35] charts. More detail is provided here.

5.1. Proposed versus Classical EWMA Chart. The proposed $THWMA_{AIB}$ chart provides superior detection ability for various values of λ against the classical EWMA chart. For instance, at $\rho = 0.75, \lambda = 0.25, \delta = 0.50$, the proposed $THWMA_{AIB}$ chart has an ARL_1 value of 7.74, while the classical EWMA chart has an ARL_1 value of 47.36 (see Tables 2 and 5). The supremacy of the proposed $THWMA_{AIB}$ chart compared to the classical EWMA chart can be seen in Figure 1. Evaluating the overall efficiency with $\lambda = 0.10$, the $THWMA_{AIB}$ chart has smaller EQL, RARL, and PCI (i.e., 9.38, 1.000, 1.000) values against the classical EWMA chart EQL, RARL, and PCI (i.e., 13.38, 1.43, 2.23) values (see Table 6).

5.2. Proposed versus TEWMA Chart. The proposed $THWMA_{AIB}$ chart is superior to the $TEWMA$ chart. For example, at $\delta = 0.25$, the proposed $THWMA_{AIB}$ chart ($\lambda = 0.10, \rho = 0.50$) yields $ARL_1 = 13.34$, whereas the $TEWMA$ chart gives ARL_1 equal to 74.21 (see Table 1 and 5). The superiority of the $THWMA_{AIB}$ chart than the $TEWMA$ chart can also be found in Figure 1. Additionally, for a specific range of shifts, the EQL, RARL, and PCI values for proposed $THWMA_{AIB}$ chart are smaller than the $TEWMA$ chart. For example, at $\lambda = 0.50$, for $THWMA_{AIB}$ and $TEWMA$ charts, the EQL, RARL, and PCI values are (13.03, 1.000, 1.000) and (15.29, 1.26, 1.17), respectively (see Table 6).

5.3. Proposed versus MHC Chart. The proposed $THWMA_{AIB}$ chart is better for tracking changes in process location than the MHC chart. For example, with $\lambda = 0.10$ and $\delta = 0.25, 0.50, 0.75$, the ARL_1 values of the MHC chart are (25.00, 13.00, 9.00), while the ARL_1 values of proposed $THWMA_{AIB}$ chart ($\rho = 0.50$) are (13.34, 6.01, 3.83) (see Table 1 and 5). Figure 1 also highlighted the dominant position of the $THWMA_{AIB}$ chart on the MHC chart. Also, the EQL, PCI, and RARL values are significantly higher for the MHC chart as compared to $THWMA_{AIB}$ chart. For illustration, at $\lambda = 0.25$, the $THWMA_{AIB}$ chart has $EQL = 10.35$, $PCI = 1.00$, and $RARL = 1.00$, whereas the MHC chart has $EQL = 22.05$, $PCI = 2.13$, and $RARL = 1.98$ measures (see Table 6).

5.4. Proposed versus $EWMA_{AIB}$ Chart. The proposed $THWMA_{AIB}$ chart offers good performance against the $EWMA_{AIB}$ chart. As an illustration, at $\lambda = 0.10, \rho = 0.50$ and $\delta \in (0.25, 0.50)$, the ARL_1 (80.66, 22.04) values of the $EWMA_{AIB}$ chart are larger than the ARL_1 (13.34, 6.01) values of the $THWMA_{AIB}$ chart (see Tables 1 and 5). Visual

TABLE 1: ARL values of the proposed THWMA_{AIB} chart for $\lambda = 0.10$ and $ARL_0 = 500$.

ρ	δ	$L_{THWMA_{AIB}} = 1.2855$												
		0.00	0.05	0.10	0.20	0.25	0.50	0.75	1.00	1.50	2.00	2.50	3.00	5.00
0.00	ARL	501.48	102.71	39.14	23.32	17.03	7.81	4.66	3.50	2.15	1.54	1.23	1.10	1.00
	SDRL	2641.60	340.71	88.06	39.85	26.72	8.66	4.29	2.63	1.52	0.99	0.66	0.44	0.00
	MDRL	9.000	9.000	7.000	8.000	7.000	5.00	4.00	3.00	1.00	1.00	1.00	1.00	1.00
0.25	ARL	503.18	94.35	43.72	23.50	17.40	7.35	4.75	3.36	2.17	1.49	1.23	1.06	1.00
	SDRL	2862.44	320.47	90.37	39.81	26.07	7.74	4.08	2.54	1.52	0.95	0.67	0.35	0.00
	MDRL	8.000	8.500	9.00	8.00	7.000	5.00	4.00	3.00	1.00	1.00	1.00	1.00	1.00
0.50	ARL	501.16	80.26	37.62	17.25	13.34	6.01	3.83	2.80	1.80	1.32	1.11	1.03	1.00
	SDRL	2702.05	252.82	84.76	27.86	19.37	6.07	3.21	2.09	1.23	0.78	0.46	0.24	0.00
	MDRL	8.000	8.000	7.000	6.00	6.000	4.00	3.00	3.00	1.00	1.00	1.00	1.00	1.00
0.75	ARL	503.05	65.89	28.36	12.04	9.670	4.39	2.93	2.11	1.35	1.08	1.01	1.00	1.00
	SDRL	2603.27	188.89	61.46	16.12	11.84	3.84	2.29	1.49	0.81	0.40	0.14	0.09	0.00
	MDRL	8.000	8.000	6.00	6.00	5.00	4.00	3.00	1.00	1.00	1.00	1.00	1.00	1.00
0.90	ARL	503.10	37.59	17.97	8.21	6.09	2.87	1.83	1.37	1.04	1.00	1.00	1.00	1.00
	SDRL	2658.15	75.79	30.21	8.81	6.82	2.14	1.28	0.83	0.29	0.06	0.00	0.00	0.00
	MDRL	7.000	8.000	6.00	5.00	4.00	3.00	1.00	1.00	1.00	1.00	1.00	1.00	1.00
0.95	ARL	501.31	26.85	11.17	5.68	4.11	2.00	1.27	1.05	1.00	1.00	1.00	1.00	1.00
	SDRL	2733.71	49.49	13.86	5.35	3.60	1.39	0.70	0.31	0.00	0.00	0.00	0.00	0.00
	MDRL	8.000	7.000	6.00	4.00	3.00	1.00	1.00	1.00	1.00	1.00	1.00	1.00	1.00

TABLE 2: ARL values of the proposed THWMA_{AIB} chart for $\lambda = 0.25$ and $ARL_0 = 500$.

ρ	δ	$L_{THWMA_{AIB}} = 1.900$												
		0.00	0.05	0.10	0.20	0.25	0.50	0.75	1.00	1.50	2.00	2.50	3.00	5.00
0.00	ARL	503.61	319.46	161.79	61.69	44.24	14.52	7.79	5.18	3.05	2.11	1.58	1.27	1.00
	SDRL	612.20	400.52	194.95	68.22	47.11	13.26	6.12	3.63	1.90	1.33	0.98	0.69	0.06
	MDRL	226.00	153.00	89.00	38.00	28.00	10.00	6.00	4.00	3.00	1.00	1.00	1.00	1.00
0.25	ARL	502.50	313.03	155.76	58.77	42.01	13.84	7.42	4.93	2.93	2.03	1.51	1.23	1.00
	SDRL	610.66	391.94	186.75	64.52	44.50	12.50	5.77	3.42	1.83	1.27	0.93	0.64	0.04
	MDRL	225.00	153.00	86.00	36.00	27.00	10.00	6.00	4.00	3.00	1.00	1.00	1.00	1.00
0.50	ARL	501.40	286.40	134.75	50.20	35.07	11.65	6.31	4.26	2.54	1.75	1.32	1.11	1.00
	SDRL	609.85	358.25	159.45	53.94	36.40	10.15	4.68	2.83	1.58	1.10	0.75	0.45	0.02
	MDRL	223.00	142.00	76.00	32.00	23.00	9.00	5.00	4.00	3.00	1.00	1.00	1.00	1.00
0.75	ARL	504.97	221.98	93.37	32.66	22.83	7.74	4.38	3.02	1.79	1.26	1.06	1.01	1.00
	SDRL	610.64	274.09	106.55	33.71	22.43	6.07	2.93	1.88	1.12	0.68	0.32	0.11	0.00
	MDRL	230.00	115.00	56.00	21.00	15.00	6.00	4.00	3.00	1.00	1.00	1.00	1.00	1.00
0.90	ARL	502.67	135.40	50.06	16.71	11.75	4.32	2.56	1.77	1.12	1.01	1.00	1.00	1.00
	SDRL	611.51	159.99	53.92	15.58	10.28	2.87	1.59	1.11	0.47	0.11	0.01	0.00	0.00
	MDRL	230.00	76.00	31.00	12.00	9.00	4.00	3.00	1.00	1.00	1.00	1.00	1.00	1.00
0.95	ARL	503.71	86.19	29.81	9.87	7.10	2.81	1.66	1.19	1.00	1.00	1.00	1.00	1.00
	SDRL	612.43	97.80	30.48	8.25	5.45	1.75	1.04	0.58	0.08	0.00	0.00	0.00	0.00
	MDRL	229.00	51.00	20.00	8.00	6.00	3.00	1.00	1.00	1.00	1.00	1.00	1.00	1.00

representation confirms the supremacy of the proposed THWMA_{AIB} chart over EWMA_{AIB} chart (see Figure 2). The dominance of the THWMA_{AIB} chart against the EWMA_{AIB} chart is seen in the EQL, RARL, and PCI values for a certain range of shifts. As an illustration, at $\lambda = 0.10$, the proposed THWMA_{AIB} chart has EQL = 9.38, PCI = 1.00, and RARL = 1.00, while the EWMA_{AIB} chart has EQL = 11.78, PCI = 1.26, RARL = 1.82 (see Table 6). This reveals the superiority of the proposed THWMA_{AIB} chart.

5.5. *Proposed versus HWMA Chart.* The proposed THWMA_{AIB} chart has lower ARL₁ values than the HWMA chart. Suppose that, for $\lambda = 0.50$, $\delta = 0.25$, the ARL₁ value of

the proposed THWMA_{AIB} chart with $\rho = 0.50$ is 68.01, while the ARL₁ value of the HWMA chart is 218.06 (see Tables 3 and 5). In other words, the proposed chart can track a quick shift in the process parameter than the HWMA chart (see Figure 3). The overall performance metrics suggest that the effectiveness of proposed THWMA_{AIB} than the HWMA chart. For instance, at $\lambda = 0.50$, the EQL values for HWMA and DHWMA_{AIB} are 16.25 and 13.03, respectively (see Table 6).

5.6. *Proposed versus DHWMA Chart.* The proposed THWMA_{AIB} chart is better as compared to the DHWMA chart. As an illustration, if $\lambda = 0.10$, $\delta = 0.25$, the values of

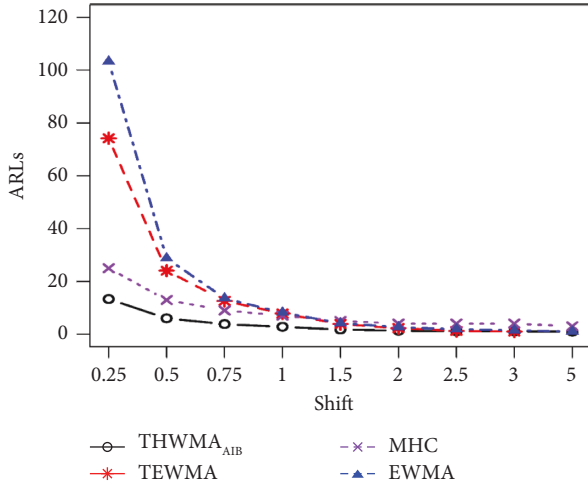


FIGURE 1: ARL comparison of the proposed THWMA_{AIB} versus classical EWMA, TEWMA, and MHC charts when $\lambda = 0.1$ and $ARL_0 = 500$.

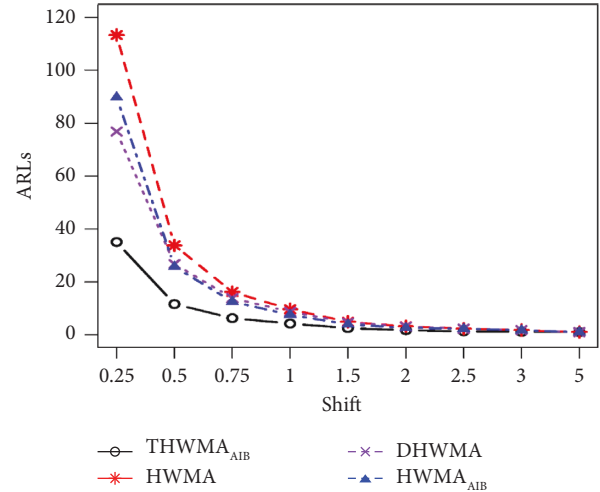


FIGURE 3: ARL comparison of the proposed THWMA_{AIB} versus HWMA, DHWMA, and HWMA_{AIB} charts when $\lambda = 0.25$ and $ARL_0 = 500$.

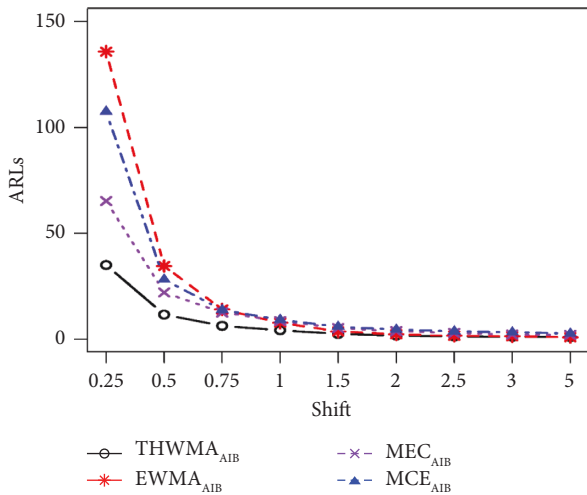


FIGURE 2: ARL comparison of the proposed THWMA_{AIB} versus EWMA, MEC_{AIB}, and MCE_{AIB} charts when $\lambda = 0.25$ and $ARL_0 = 500$.

ARL_1 for DHWMA and THWMA_{AIB} ($\rho = 0.25$) are 34.76 and 17.40, respectively (see Table 1 versus Table 5 and Figure 3). The overall performance measures highlight the superiority of the THWMA_{AIB} chart. For instance, at $\lambda = 0.10$, the EQL, PCI, and RARL values of the DHWMA and THWMA_{AIB} charts are presented as (10.76, 1.15, and 1.38), and (9.38, 1.000, and 1.000), respectively (see Table 6).

5.7. Proposed versus HWMA_{AIB} Chart. The proposed THWMA_{AIB} chart detects earlier shift than the HWMA_{AIB} chart. If $\lambda = 0.10$, $\rho = 0.50$, and $\delta = (0.25, 0.50, 0.75)$ the ARL_1 values of the charts are (65.89, 22.63, 11.79) and (13.34, 6.01, 3.83) respectively, for HWMA_{AIB} and THWMA_{AIB}

charts (see Tables 1 and 5). Figure 3 also reveals the better performance of the proposed THWMA_{AIB} against the HWMA_{AIB} chart. Likewise, the HWMA_{AIB} chart EQL, RARL, and PCI (i.e., 14.55, 1.12, and 1.23) values are higher than the EQL, RARL, and PCI (13.03, 1.000, and 1.000) values of the THWMA_{AIB} chart at $\lambda = 0.50, \rho = 0.50$ (see Table 6).

5.8. Proposed versus MEC_{AIB} Chart. By comparing the ARL measures, the proposed THWMA_{AIB} chart with the MEC_{AIB} chart shows that the THWMA_{AIB} chart is more sensitive for all δ and λ values. For instance, with $\lambda = 0.25, \rho = 0.50$, $\delta = 0.25, 0.50, 0.75$, the $ARL_1 = 35.07, 11.65, 6.31$ for THWMA_{AIB} chart, while the ($ARL_1 = 65.26, 22.14, 12.61$) for MEC_{AIB} ($k = 0.50$) chart (see Tables 2 and 5). The proposed THWMA_{AIB} chart has smaller EQL, RARL, and PCI measures as compared to the MEC_{AIB} chart (see Table 6). Figure 2 illustrates that the proposed THWMA_{AIB} is functioning well and detects shifts earlier in the process. These findings demonstrate that the proposed THWMA_{AIB} chart performs better than the MEC_{AIB} chart.

5.9. Proposed versus MCE_{AIB} Chart. The ARL study indicates that the proposed THWMA_{AIB} chart works much better than the MCE_{AIB} chart for each of the choices formed by λ, δ (see Tables 1–4 versus 5). As an illustration, Table 3 and 5 shows that at ($\lambda = 0.50, \delta = (0.25, 0.50, 0.75), \rho = 0.50$), the ARL_1 values of the proposed THWMA_{AIB} chart are (68.01, 23.02, 11.93), and the corresponding values of ARL_1 for MCE_{AIB} chart ($k = 0.50$) are (111.47, 28.62, 13.55). Figure 2 indicates that the proposed THWMA_{AIB} chart is better than the MCE_{AIB} chart. In the overall performance scenario, the proposed THWMA_{AIB} chart also exhibits overperformance than MCE_{AIB} chart (see Table 6).

TABLE 3: ARL values of the proposed THWMA_{AIB} chart for $\lambda = 0.50$ and $ARL_0 = 500$.

ρ	δ	$L_{THWMA_{AIB}} = 2.992$												
		0.00	0.05	0.10	0.20	0.25	0.50	0.75	1.00	1.50	2.00	2.50	3.00	5.00
0.00	ARL	499.25	401.97	259.88	115.66	84.14	29.02	15.03	9.45	5.00	3.33	2.45	1.88	1.03
	SDRL	428.13	344.00	216.62	87.43	61.14	18.37	8.78	5.20	2.42	1.52	1.17	0.98	0.18
	MDRL	387.00	311.00	202.00	95.00	70.00	25.00	13.00	9.00	5.00	3.00	3.00	1.00	1.00
0.25	ARL	496.96	396.92	251.97	110.33	80.30	27.49	14.36	8.97	4.76	3.18	2.35	1.79	1.02
	SDRL	427.47	339.79	210.10	83.17	57.95	17.21	8.31	4.89	2.29	1.45	1.14	0.94	0.15
	MDRL	384.00	306.00	197.00	90.50	67.00	24.00	13.00	8.00	4.00	3.00	3.00	1.00	1.00
0.50	ARL	498.49	378.78	226.01	94.11	68.01	23.02	11.93	7.50	4.06	2.75	1.99	1.50	1.00
	SDRL	428.74	325.16	186.07	69.40	47.70	14.12	6.76	3.97	1.89	1.27	1.02	0.79	0.06
	MDRL	384.00	291.00	177.00	78.00	58.00	20.00	11.00	7.00	4.00	3.00	2.00	1.00	1.00
0.75	ARL	498.97	324.43	166.97	63.23	45.01	14.81	7.71	4.96	2.81	1.86	1.32	1.08	1.00
	SDRL	427.80	276.15	133.22	44.19	29.98	8.64	4.13	2.41	1.30	0.97	0.65	0.32	0.00
	MDRL	385.00	251.00	133.00	53.00	39.00	13.00	7.00	5.00	3.00	1.00	1.00	1.00	1.00
0.90	ARL	498.09	227.88	95.21	33.33	23.29	7.57	4.11	2.76	1.52	1.07	1.00	1.00	1.00
	SDRL	428.96	188.01	70.38	21.35	14.30	4.03	1.91	1.28	0.80	0.30	0.06	0.01	0.00
	MDRL	387.00	179.00	79.00	29.00	21.00	7.00	4.00	3.00	1.00	1.00	1.00	1.00	1.00
0.95	ARL	498.09	155.14	58.13	19.54	13.54	4.55	2.60	1.70	1.04	1.00	1.00	1.00	1.00
	SDRL	428.96	155.14	58.13	19.54	13.54	4.55	2.60	1.70	1.04	1.00	1.00	1.00	1.00
	MDRL	387.00	123.01	40.07	11.73	7.83	2.17	1.22	0.90	0.23	0.02	0.00	0.00	0.00

TABLE 4: ARL values of the proposed THWMA_{AIB} chart for $\lambda = 0.75$ and $ARL_0 = 500$.

ρ	δ	$L_{THWMA_{AIB}} = 3.086$												
		0.00	0.05	0.10	0.20	0.25	0.50	0.75	1.00	1.50	2.00	2.50	3.00	5.00
0.00	ARL	499.00	472.53	394.17	240.47	181.18	54.11	22.27	11.89	5.22	3.11	2.19	1.68	1.03
	SDRL	496.67	471.44	391.22	234.98	175.61	48.78	18.26	8.84	3.22	1.64	1.04	0.74	0.16
	MDRL	347.00	328.00	275.00	169.00	128.00	40.00	17.00	10.00	4.00	3.00	2.00	2.00	1.00
0.25	ARL	499.12	467.64	390.36	231.45	173.26	49.91	20.81	11.15	4.90	2.97	2.09	1.61	1.02
	SDRL	494.39	465.74	385.16	227.52	166.18	44.87	16.85	8.24	2.96	1.53	0.98	0.70	0.13
	MDRL	347.00	323.00	273.00	163.00	123.00	37.00	16.00	9.00	4.00	3.00	2.00	1.00	1.00
0.50	ARL	498.26	459.87	370.16	202.16	146.83	39.62	16.31	8.77	4.00	2.47	1.77	1.39	1.00
	SDRL	495.53	458.28	367.02	195.49	140.86	34.93	12.77	6.10	2.27	1.21	0.80	0.57	0.06
	MDRL	346.00	319.00	258.00	143.00	104.00	30.00	13.00	7.00	4.00	2.00	2.00	1.00	1.00
0.75	ARL	498.33	434.97	311.17	137.44	93.19	21.96	9.09	5.14	2.55	1.67	1.26	1.08	1.00
	SDRL	494.82	433.55	306.48	131.90	87.31	17.94	6.38	3.14	1.26	0.74	0.47	0.27	0.00
	MDRL	347.00	303.00	217.00	98.00	67.00	17.00	7.00	4.00	2.00	2.00	1.00	1.00	1.00
0.90	ARL	499.04	371.46	204.36	63.92	40.24	8.90	4.05	2.50	1.41	1.07	1.00	1.00	1.00
	SDRL	496.89	368.42	199.16	58.41	35.42	6.23	2.32	1.22	0.58	0.25	0.07	0.01	0.00
	MDRL	348.00	259.00	144.00	47.00	30.00	7.00	4.00	2.00	1.00	1.00	1.00	1.00	1.00
0.95	ARL	498.05	297.88	124.69	31.76	19.36	4.61	2.33	1.54	1.04	1.00	1.00	1.00	1.00
	SDRL	494.39	293.94	119.67	27.28	15.50	2.73	1.12	0.66	0.20	0.02	0.00	0.00	0.00
	MDRL	347.50	208.00	89.00	24.00	15.00	4.00	2.00	1.00	1.00	1.00	1.00	1.00	1.00

5.10. *Main Findings of the Study.* Important findings of the proposed THWMA_{AIB} chart are listed below:

- (i) The THWMA_{AIB} statistic improves the detection ability of the proposed chart.
- (ii) The efficiency of the proposed THWMA_{AIB} chart is strengthened with the appropriate inclusion of auxiliary information in the structure (see Tables 1–5).

- (iii) Unlike the classic CUSUM, MHC, EWMA, HWMA, DHWMA, HWMA_{AIB}, EWMA_{AIB}, MEC_{AIB} and MCE_{AIB} charts, the ARL₁ values of the proposed THWMA_{AIB} chart are smaller at various parameter values.

- (iv) Overall performance evaluations demonstrate that the THWMA_{AIB} chart is dominant over the other competing charts included in this research (see Subsections 5.1–5.9).

TABLE 5: ARL values of some existing charts when $ARL_0 = 500$.

	δ									
	0.00	0.25	0.50	0.75	1.00	1.50	2.00	2.50	3.00	5.00
	$\lambda = 0.10$									
TEWMA	499.31	74.21	24.05	12.63	7.85	3.85	2.29	1.77	1.25	1.00
MHC ($k = 0.50$)	501.00	25.00	13.00	9.00	7.00	5.00	4.00	4.00	4.00	3.00
EWMA	500.00	103.32	28.81	13.61	8.21	4.17	2.66	1.92	1.51	1.02
HWMA	500.00	81.48	28.61	14.85	9.35	4.98	3.32	2.45	1.87	1.03
DHWMA	499.10	34.76	11.97	6.63	4.56	2.72	1.93	1.46	1.19	1.00
HWMA _{AIB} ($\rho = 0.50$)	501.47	65.89	22.63	11.79	7.43	4.04	2.72	2.43	1.83	1.01
EWMA _{AIB} ($\rho = 0.50$)	499.81	80.66	22.04	10.54	6.43	3.32	2.15	1.58	1.28	1.00
MEC _{AIB} ($\rho = 0.50, k = 0.50$)	500.63	56.29	19.98	11.42	7.73	4.38	3.00	2.00	2.00	1.00
MCE _{AIB} ($\rho = 0.50, k = 0.50$)	499.47	100.25	27.98	14.51	10.20	6.77	5.29	4.43	3.87	3.12
	$\lambda = 0.25$									
TEWMA	500.31	110.74	30.04	13.96	8.49	4.35	2.69	2.02	1.43	1.05
MHC ($k = 0.50$)	499.00	31.00	12.00	8.00	6.00	4.00	4.00	3.00	3.00	2.00
EWMA	500.00	169.34	47.36	19.31	10.41	4.78	2.94	2.09	1.62	1.02
HWMA	500.00	113.34	33.79	16.19	9.71	4.94	3.20	2.33	1.79	1.03
DHWMA	501.37	76.86	26.77	13.88	8.69	4.66	3.12	2.32	1.77	1.02
HWMA _{AIB} ($\rho = 0.50$)	504.88	89.86	25.77	12.52	7.59	3.95	2.61	2.30	1.75	1.01
EWMA _{AIB} ($\rho = 0.50$)	499.69	135.77	34.58	14.11	7.80	3.72	2.35	1.70	1.35	1.00
MEC _{AIB} ($\rho = 0.50, k = 0.50$)	498.72	65.26	22.14	12.61	8.65	5.32	3.80	2.99	2.24	1.99
MCE _{AIB} ($\rho = 0.50, k = 0.50$)	500.69	107.49	28.22	13.83	9.24	5.93	4.56	3.79	3.30	2.71
	$\lambda = 0.50$									
TEWMA	500.80	173.21	48.31	19.31	10.19	4.63	2.85	2.19	1.57	1.15
MHC ($k = 0.50$)	501.00	52.00	16.00	9.00	6.00	4.00	3.00	3.00	3.00	2.00
EWMA	500.00	254.53	88.43	35.57	17.18	6.27	3.39	2.26	1.70	1.03
HWMA	500.00	218.06	69.04	27.87	14.08	5.67	3.20	2.20	1.68	1.03
DHWMA	502.39	113.02	34.29	16.38	9.78	4.95	3.19	2.32	1.78	1.03
HWMA _{AIB} ($\rho = 0.50$)	498.55	180.91	50.43	19.87	10.06	4.21	2.50	2.17	1.64	1.01
EWMA _{AIB} ($\rho = 0.50$)	500.79	216.10	65.40	24.80	11.91	4.56	2.59	1.80	1.40	1.00
MEC _{AIB} ($\rho = 0.50, k = 0.50$)	502.77	77.88	23.42	12.53	8.45	5.16	3.76	3.01	2.43	1.01
MCE _{AIB} ($\rho = 0.50, k = 0.50$)	500.11	111.47	28.62	13.55	8.65	5.26	3.93	3.24	2.80	2.16

TABLE 6: EQL, PCI, and RARL measures of the proposed versus existing charts.

	$\lambda = 0.10$									
	THWMA	MHC	EWMA	HWMA	DHWMA	HWMA _{AIB}	EWMA _{AIB}	MEC _{AIB}	MCE _{AIB}	THWMA _{AIB}
EQL	12.18	30.24	13.38	15.07	10.76	14.06	11.78	14.26	32.55	9.38
PCI	1.30	3.22	1.43	1.61	1.15	1.50	1.26	1.52	3.47	1.00
RARL	1.93	3.04	2.23	2.42	1.38	2.11	1.82	2.09	3.84	1.00
	$\lambda = 0.25$									
EQL	13.54	22.05	14.75	14.99	14.45	13.88	12.72	21.06	28.27	10.35
PCI	1.31	2.13	1.43	1.45	1.40	1.34	1.23	2.04	2.73	1.00
RARL	1.58	1.98	1.89	1.79	1.65	1.57	1.53	2.02	2.64	1.00
	$\lambda = 0.50$									
EQL	15.29	21.79	17.34	16.25	14.97	14.55	14.42	16.59	23.62	13.03
PCI	1.17	1.67	1.33	1.25	1.15	1.12	1.11	1.27	1.81	1.00
RARL	1.26	1.45	1.61	1.45	1.21	1.23	1.28	1.29	1.65	1.00

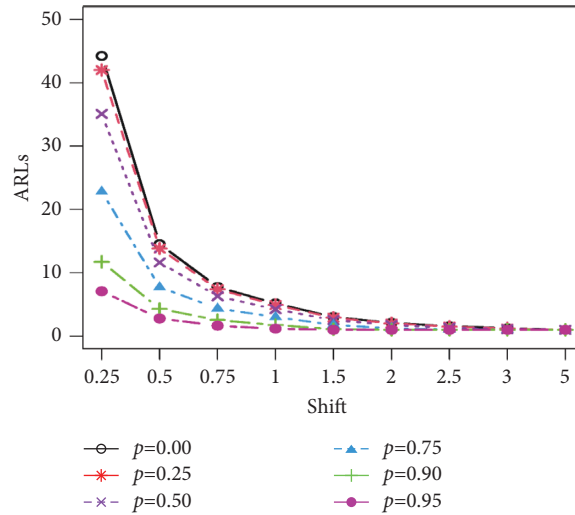


FIGURE 4: ARL comparison of the proposed THWMA_{AIB} chart for various ρ when $\lambda = 0.25$ and $ARL_0 = 500$.

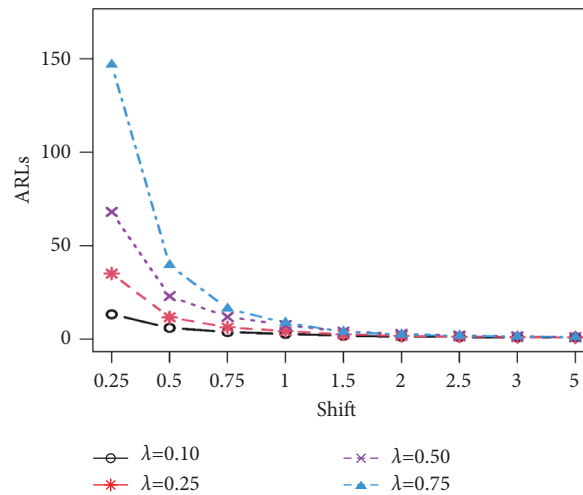


FIGURE 5: ARL comparison of the proposed THWMA_{AIB} chart for various λ when $\rho = 0.50$ and $ARL_0 = 500$.

- (v) The proposed THWMA_{AIB} chart provides optimal results for larger values ρ .
- (vi) The efficiency of the ARL_1 measures is increased by using the proposed THWMA_{AIB} chart.
- (vii) As λ increases, the control limit coefficient ($L_{THWMA_{AIB}}$) of the proposed THWMA_{AIB} chart also increases.
- (viii) The proposed THWMA_{AIB} chart is more effective for larger ρ and smaller λ in term of ARL_1 performance (see Figures 4 and 5). For example, the minimal value of ARL_1 is 4.11 at $\delta = 0.25$, $\lambda = 0.10$, and $\rho = 0.95$.

6. Case Study

This section contains the case study of the THWMA_{AIB} versus DHWMA, HWMA_{AIB} and HWMA charts. In this regard, a data set is considered from the study of Constable, et al. [39]. The data represents the measurements for

adjacent parts of the braking system of vehicles, which contains the study variable Y and auxiliary variable X . Forty-five data values are taken from the IC process, and this data set is used to estimate unknown parameters. These estimates are given as; $\bar{X} = 210.24$, $\bar{Y} = 210.18$, $s_X = 1.23$, $s_Y = 1.17$, and $r = 0.54$. In view of these estimates as the known parameters, two datasets were generated from a BND. Data set-I consists of fifteen samples with $\mu_X = 210.24$, $\mu_Y = 201.18$, $\sigma_X = 1.23$, $\sigma_Y = 1.17$ and $\rho = 0.54$ and data set-II consists of fifteen samples with $\mu_X = 210.24$, $\mu_Y = 201.88$, $\sigma_X = 1.23$, $\sigma_Y = 1.17$ and $\rho = 0.54$ (see Table 7). This fashion of perturbing the parameters in such a way can be seen from the study of Anwar, et al. [40].

For the comparison, the proposed THWMA_{AIB} chart is considered along with the existing DHWMA, HWMA_{AIB}, and HWMA charts. Furthermore, the parameters of the proposed THWMA_{AIB} chart are $L_{THWMA_{AIB}} = 1.90$, $\lambda = 0.25$, $\rho = 0.54$ with $ARL_0 = 500$, and the parameters of the DHWMA chart are $L_{DHWMA} = 2.7424$, $\lambda = 0.25$, with $ARL_0 = 500$. Likewise, the parameters of HWMA_{AIB} chart

TABLE 7: Continued.

	1	2	3	4	5	6	7	8	9	10	11	12	13	14	15
Plotting statistic	201.97	201.72	201.96	201.48	201.65	202.18	201.77	201.25	201.95	202.11	201.06	201.35	201.57	201.79	201.97
$LCL_{(HWMMA)F}$	200.58	200.59	200.6	200.6	200.61	200.61	200.62	200.62	200.62	200.63	200.63	200.63	200.64	200.64	200.64
$UCL_{(HWMMA)F}$	201.78	201.77	201.76	201.76	201.75	201.75	201.74	201.74	201.74	201.73	201.73	201.73	201.72	201.72	201.72
Plotting statistic	201.86	201.56	201.94	201.66	201.57	202.09	201.58	201.64	202	201.88	201.19	201.38	201.55	201.87	201.86
$LCL_{(HWMMA_{AIB})F}$	200.58	200.59	200.6	200.6	200.61	200.61	200.62	200.62	200.62	200.63	200.63	200.63	200.64	200.64	200.64
$UCL_{(HWMMA_{AIB})F}$	201.78	201.77	201.76	201.76	201.75	201.75	201.74	201.74	201.74	201.73	201.73	201.73	201.72	201.72	201.72
Plotting statistic	201.48	201.54	201.64	201.59	201.61	201.75	201.73	201.61	201.72	201.8	201.59	201.58	201.6	201.65	201.71
$LCL_{(DHWMA)F}$	200.76	200.77	200.78	200.79	200.8	200.81	200.82	200.83	200.84	200.84	200.85	200.85	200.86	200.86	200.87
$UCL_{(DHWMA)F}$	201.6	201.59	201.58	201.57	201.56	201.55	201.54	201.53	201.52	201.52	201.51	201.51	201.5	201.5	201.49
Plotting statistic	201.41	201.5	201.54	201.61	201.62	201.64	201.69	201.68	201.69	201.74	201.72	201.65	201.62	201.63	201.66
$LCL_{(THWMA_{AIB})F}$	200.93	200.94	200.95	200.95	200.96	200.96	200.97	200.97	200.98	200.98	200.99	200.99	200.99	201	201
$UCL_{(THWMA_{AIB})F}$	201.43	201.42	201.41	201.41	201.4	201.4	201.39	201.39	201.38	201.38	201.37	201.37	201.37	201.36	201.36

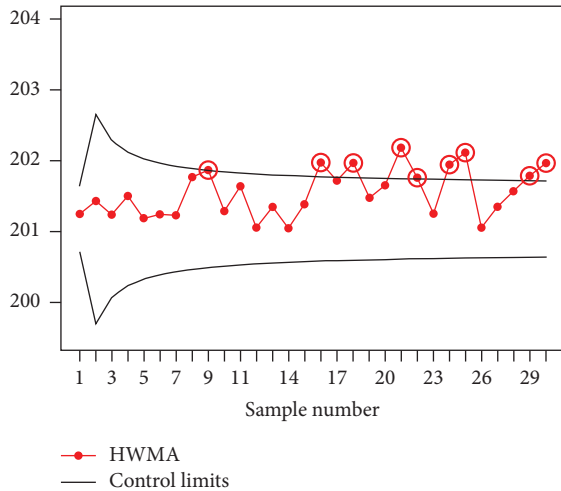


FIGURE 6: Application for the existing HWMA chart when $L_{HWMA} = 3.075$, $\lambda = 0.25$ and $ARL_0 = 500$.

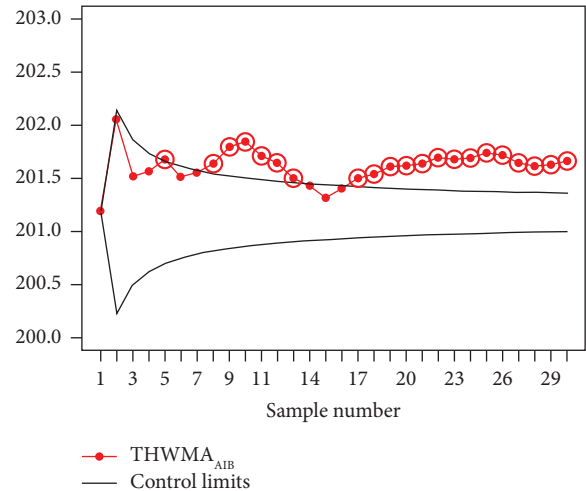


FIGURE 9: Application for the proposed $THWMA_{AIB}$ chart when $L_{THWMA_{AIB}} = 1.90$, $\lambda = 0.25$, $\rho = 0.54$, and $ARL_0 = 500$.

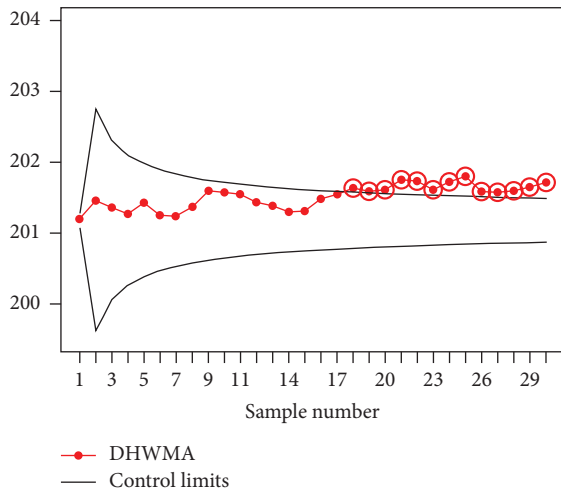


FIGURE 7: Application for the existing DHWMA chart when $L_{DHWMA} = 2.7424$, $\lambda = 0.25$ and $ARL_0 = 500$.

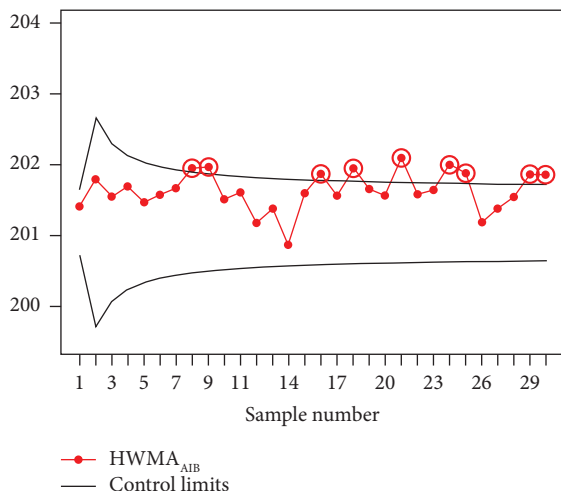


FIGURE 8: Application for the existing $HWMA_{AIB}$ chart when $L_{HWMA_{AIB}} = 3.075$, $\lambda = 0.25$, $\rho = 0.54$, and $ARL_0 = 500$.

are $L_{THWMA_{AIB}} = 1.90, \lambda = 0.25, \rho = 0.54$ with $ARL_0 = 500$, and the parameters of the HWMA chart are $L_{HWMA} = 3.075, \lambda = 0.25$, with $ARL_0 = 500$. From Table 7 and Figures 6–9 the proposed $THWMA_{AIB}$ chart tracks the first OOC signal at the 5th sample, whereas the DHWMA, $HWMA_{AIB}$, and HWMA charts track the first OOC signal at the 18th, 8th, and 9th samples, respectively. Overall, the proposed $THWMA_{AIB}$ chart highlights 21 OOC points, while the DHWMA, $HWMA_{AIB}$, and HWMA charts highlight 13, 9, and 9 OOC points, respectively. This shows that the proposed $THWMA_{AIB}$ chart is more sensitive than the existing DHWMA, $HWMA_{AIB}$, and HWMA charts.

7. Summary, Conclusions, And Recommendations

The objective of this study is to enhance homogeneously weighted moving average (HWMA) and double HWMA (DHWMA) charts and propose an auxiliary-information-based triple HWMA, symbolized as $THWMA_{AIB}$ chart to further improve the process location shift monitoring. To evaluate the performance of the proposed $THWMA_{AIB}$ chart against other charts, an algorithm is developed in R software using the Monte Carlo simulation technique to obtain numerical results. The analysis based on average run length, extra quadratic loss, performance comparison index, and relative average run length reveals the proposed $THWMA_{AIB}$ chart over-performed against EWMA, $EWMA_{AIB}$, HWMA, $HWMA_{AIB}$, DHWMA, TEWMA, MCE_{AIB} , MEC_{AIB} and MHC charts. Finally, to demonstrate the proposed $THWMA_{AIB}$ chart's utility from a practical perspective, a real-world application is included. This study can be extended for multivariate and more than one auxiliary characteristic in the model.

Data Availability

The data used to support the findings of this study are available from the corresponding author upon request.

Conflicts of Interest

The authors declare that they have no conflicts of interest.

Authors' Contributions

Conceptualization (Syed Masroor Anwar, Zahid Rasheed). Formal Analysis (Syed Masroor Anwar, Nafiu Lukman Abiodun). Funding Acquisition (Somayya Komal, Ammara Nawaz Cheema). Investigation (Somayya Komal, Ammara Nawaz Cheema). Methodology (Syed Masroor Anwar, Majid Khan). Project Administration (Nafiu Lukman Abiodun, Majid Khan). Resources (Somayya Komal, Zahid Rasheed). Supervision (Nafiu Lukman Abiodun, Majid Khan). Validation (Somayya Komal, Ammara Nawaz Cheema). Visualization (Syed Masroor Anwar, Zahid Rasheed). Writing–Original Draft Preparation (Syed Masroor Anwar, Nafiu Lukman Abiodun). Writing–Review and Editing (Somayya Komal, Ammara Nawaz Cheema, Zahid Rasheed).

References

- [1] W. A. Shewhart, *Economic Control of Quality of Manufactured Product*, D. Van Nostrand Company, New York, 1931.
- [2] E. S. Page, "Continuous inspection schemes," *Biometrika*, vol. 41, no. 1/2, pp. 100–115, 1954.
- [3] S. W. Roberts, "Control chart tests based on geometric moving averages," *Technometrics*, vol. 1, no. 3, pp. 239–250, 1959.
- [4] S. E. Shamma and A. K. Shamma, "Development and evaluation of control charts using double exponentially weighted moving averages," *International Journal of Quality & Reliability Management*, vol. 9, no. 6, pp. 18–25, 1992.
- [5] V. Alevizakos, K. Chatterjee, and C. Koukouvinos, "The triple exponentially weighted moving average control chart," *Quality Technology & Quantitative Management*, vol. 18, no. 3, pp. 1–29, 2020.
- [6] V. Alevizakos, K. Chatterjee, and C. Koukouvinos, "A triple exponentially weighted moving average control chart for monitoring time between events," *Quality and Reliability Engineering International*, vol. 37, no. 3, pp. 1059–1079, 2020.
- [7] S. Sukparungsee, Y. Areepong, and R. Taboran, "Exponentially weighted moving average—moving average charts for monitoring the process mean," *PLoS One*, vol. 15, no. 2, Article ID e0228208, 2020.
- [8] R. Taboran, S. Sukparungsee, and Y. Areepong, "Design of a new Tukey MA-DEWMA control chart to monitor process and its applications," *IEEE Access*, vol. 9, pp. 102746–102757, 2021.
- [9] K. Talordphop, S. Sukparungsee, and Y. Areepong, "New modified exponentially weighted moving average—moving average control chart for process monitoring," *Connection Science*, vol. 34, no. 1, pp. 1981–1998, 2022.
- [10] R. Taboran, S. Sukparungsee, and Y. Areepong, "A new nonparametric Tukey MA-EWMA control charts for detecting mean shifts," *IEEE Access*, vol. 8, pp. 207249–207259, 2020.
- [11] K. Chatterjee, C. Koukouvinos, and A. Lappa, "A new S2-TEWMA control chart for monitoring process dispersion," *Quality and Reliability Engineering International*, vol. 37, no. 4, pp. 1334–1354, 2020.
- [12] V. Alevizakos, K. Chatterjee, and C. Koukouvinos, "A non-parametric triple exponentially weighted moving average sign control chart," *Quality and Reliability Engineering International*, vol. 37, no. 4, pp. 1504–1523, 2020.
- [13] V. Alevizakos, K. Chatterjee, and C. Koukouvinos, "Non-parametric Triple Exponentially Weighted Moving Average Signed-Rank Control Chart for Monitoring Shifts in the Process Location," *Quality and Reliability Engineering International*, vol. 37, 2021.
- [14] Z. Rasheed, H. Zhang, M. Arslan et al., "An Efficient Robust Nonparametric Triple EWMA Wilcoxon Signed-Rank Control Chart for Process Location," *Mathematical Problems in Engineering*, vol. 2021, Article ID 2570198, 2021.
- [15] S. Abbasi and A. Haq, "Optimal CUSUM and adaptive CUSUM charts with auxiliary information for process mean," *Journal of Statistical Computation and Simulation*, vol. 89, no. 2, pp. 337–361, 2019.
- [16] N. Abbas, M. Riaz, and R. J. M. M. Does, "An EWMA-type control chart for monitoring the process mean using auxiliary information," *Communications in Statistics - Theory and Methods*, vol. 43, no. 16, pp. 3485–3498, 2014.
- [17] N. A. Adegoke, M. Riaz, R. A. Sanusi, A. N. Smith, and M. D. Pawley, "EWMA-type scheme for monitoring location parameter using auxiliary information," *Computers & Industrial Engineering*, vol. 114, pp. 114–129, 2017.
- [18] M. Noor-ul-Amin, S. Khan, and A. Sanaullah, "HEWMA control chart using auxiliary information," *Iranian Journal of Science and Technology Transaction A-Science*, vol. 43, no. 3, pp. 891–903, 2018.
- [19] A. Haq and M. B. C. Khoo, "Memorytype multivariate control charts with auxiliary information for process mean," *Quality and Reliability Engineering International*, vol. 35, no. 1, pp. 192–203, 2019.
- [20] S. M. Anwar, M. Aslam, S. Ahmad, and M. Riaz, "A modified-mxEWMA location chart for the improved process monitoring using auxiliary information and its application in wood industry," *Quality Technology & Quantitative Management*, vol. 17, no. 5, pp. 561–579, 2020.
- [21] M. Aslam and S. M. Anwar, "An improved Bayesian Modified-EWMA location chart and its applications in mechanical and sport industry," *PLoS One*, vol. 15, no. 2, Article ID e0229422, 2020.
- [22] S. M. Anwar, M. Aslam, M. Riaz, and B. Zaman, "On mixed memory control charts based on auxiliary information for efficient process monitoring," *Quality and Reliability Engineering International*, vol. 36, no. 6, pp. 1949–1968, 2020.
- [23] S. M. Anwar, M. Aslam, B. Zaman, and M. Riaz, "Mixed memory control chart based on auxiliary information for simultaneously monitoring of process parameters: an application in glass field," *Computers & Industrial Engineering*, vol. 156, Article ID 107284, 2021.
- [24] A. Haq, S. Akhtar, and M. Boon Chong Khoo, "Adaptive CUSUM and EWMA charts with auxiliary information and variable sampling intervals for monitoring the process mean," *Quality and Reliability Engineering International*, vol. 37, no. 1, pp. 47–59, 2021.
- [25] H. Lee, M. Aslam, Q. u. a. Shakeel, W. Lee, and C. H. Jun, "A control chart using an auxiliary variable and repetitive sampling for monitoring process mean," *Journal of Statistical Computation and Simulation*, vol. 85, no. 16, pp. 3289–3296, 2015.
- [26] A. Haq, "A new maximum EWMA control chart for simultaneously monitoring process mean and dispersion using

- auxiliary information," *Quality and Reliability Engineering International*, vol. 33, no. 7, pp. 1577–1587, 2017.
- [27] A. Haq, "A new adaptive EWMA control chart using auxiliary information for monitoring the process mean," *Communications in Statistics - Theory and Methods*, vol. 47, no. 19, pp. 4840–4858, 2018.
- [28] N. A. Adegoke, A. N. H. Smith, M. J. Anderson, R. A. Sanusi, and M. D. M. Pawley, "Efficient homogeneously weighted moving average chart for monitoring process mean using an auxiliary variable," *IEEE Access*, vol. 7, pp. 94021–94032, 2019.
- [29] J. S. Hunter, "The exponentially weighted moving average," *Journal of Quality Technology*, vol. 18, no. 4, pp. 203–210, 1986.
- [30] N. Abbas, "Homogeneously weighted moving average control chart with an application in substrate manufacturing process," *Computers & Industrial Engineering*, vol. 120, pp. 460–470, 2018.
- [31] O. A. Adeoti and S. O. Koleoso, "A hybrid homogeneously weighted moving average control chart for process monitoring," *Quality and Reliability Engineering International*, vol. 36, no. 6, pp. 2170–2186, 2020.
- [32] M. Abid, A. Shabbir, H. Z. Nazir, R. A. K. Sherwani, and M. Riaz, "A Double Homogeneously Weighted Moving Average Control Chart for Monitoring of the Process Mean," *Quality and Reliability Engineering International*, vol. 36, 2020.
- [33] M. Thanwane, S. C. Shongwe, J. C. Malela-Majika, and M. Aslam, "Parameter estimation effect of the homogeneously weighted moving average chart to monitor the mean of autocorrelated observations with measurement errors," *IEEE Access*, vol. 8, pp. 221352–221366, 2020.
- [34] M. Riaz, S. A. Abbasi, M. Abid, and A. K. Hamzat, "A new HWMA dispersion control chart with an application to wind farm data," *Mathematics*, vol. 8, no. 12, p. 2136, 2020.
- [35] M. Abid, S. Mei, H. Z. Nazir, M. Riaz, and S. Hussain, "A mixed HWMA-CUSUM mean chart with an application to manufacturing process," *Quality and Reliability Engineering International*, vol. 37, no. 2, pp. 618–631, 2021.
- [36] Z. Rasheed, H. Zhang, S. M. Anwar, and B. Zaman, "Homogeneously mixed memory charts with application in the substrate production process," *Mathematical Problems in Engineering*, vol. 2021, Article ID 2582210, 15 pages, 2021.
- [37] Z. Wu, J. Jiao, M. Yang, Y. Liu, and Z. Wang, "An enhanced adaptive CUSUM control chart," *IIE Transactions*, vol. 41, no. 7, pp. 642–653, 2009.
- [38] Y. Ou, Z. Wu, and F. Tsung, "A comparison study of effectiveness and robustness of control charts for monitoring process mean," *International Journal of Production Economics*, vol. 135, no. 1, pp. 479–490, 2012.
- [39] G. K. Constable, M. J. Cleary, C. Tickel, and G. X. Zhang, "Use of Cause-Selecting Charts in the Auto Industry," *ASQC Quality Congress Transactions*, vol. 42, pp. 597–602, 1988.
- [40] S. M. Anwar, M. Aslam, B. Zaman, and M. Riaz, "An Enhanced Double Homogeneously Weighted Moving Average Control Chart to Monitor Process Location with Application in Automobile Field," *Quality and Reliability Engineering International*, vol. 38, 2022.